

93-123



сообщения  
объединенного  
института  
ядерных  
исследований  
дубна

E10-93-123

A.A.Glazov, I.V.Kisel, G.A.Ososkov

RECONSTRUCTION OF Z-COORDINATES  
OF TRACKS IN THE ARES FACILITY

1993

# 1 Introduction

Spatial reconstruction of tracks is an important part of data processing in high energy physics. It usually consists of two stages following specific features of an experimental setup:

- recognition of tracks in  $XY$  projection (perpendicular to the magnetic field);
- reconstruction of  $Z$ -coordinates (along the magnetic field) of tracks.

Here we consider methods of  $Z$ -coordinate reconstruction in proportional strip chambers of the ARES facility [1].

The main coordinate detectors of the ARES spectrometer are 18 coaxial cylindrical multiwire proportional chambers. These chambers are of two types: chambers of the first type register only the azimuthal coordinate, but chambers of the second type (chambers 1, 4 and 9) are dual-coordinate — they register the azimuthal and axis ( $Z$ ) coordinates. The azimuthal coordinate in the proportional chambers of both types is determined by the number (position) of the hit wire, but the radial coordinate is determined by the radius of the chamber. Cathodes in the dual-coordinate chambers are solid cylinders on which there are helicoidal strips. Strips are made from aluminum foil and are wound with angle about  $30^\circ$  or  $45^\circ$  along the cylinder axis. Directions of strip winding on the inner and outer cathodes are contrary. Treatment of strip signals gives us full information about axis and azimuthal coordinates of the event. The axis ( $Z$ ) coordinate is determined by a point of intersection of the hit wire with the corresponding strips.

Obviously,  $Z$ -coordinates of tracks have to be known as accurately as possible. But there are some difficulties arising from the ARES construction. The most significant of them are:

- Almost each pair of strips crosses twice (fig. 1 shows only one pair of strips and only one anode wire).
- Strip readout system have ADC with only 256 channels, which often leads to over- and underflows.
- Due to the comparatively small number of strips on the first chamber adjacent peaks are often merged.

These difficulties together with not very high strip chamber efficiency of the ARES facility make reconstruction of correct  $Z$ -coordinates very complicated. The main non-devised problem appeared at a stage of joining up

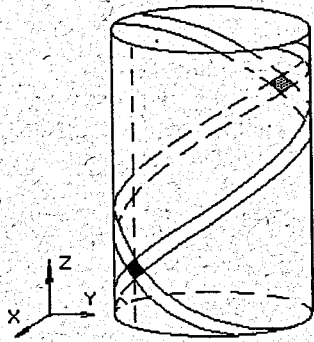


Figure 1: A scheme of ARES strip chamber.

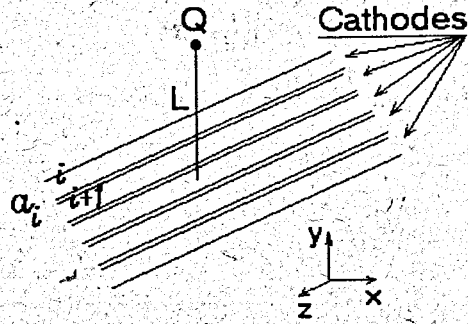


Figure 2: View of a charge and strips disposition.

Z-coordinates with XY-tracks (a problem of Z-identification). To resolve them we propose to use information about the total induced charge (TIC) in addition to known standard methods [3, 4, 5, 6]. On the basis of TIC information we construct some new effective algorithms of Z-coordinate reconstruction. These algorithms are tested on real  $\mu \rightarrow 3e$  and  $\pi \rightarrow 3e\nu$  events obtained on the ARES setup [2]. The results of the test are quite successful.

## 2 The physical basis

The thorough analysis of physical processes in proportional chambers with strip read-out can be found in [3, 4, 5]. They are summarized as follows:

- As a result of track passing through a chamber, gas ionization takes place.
- Electrons drift to anode wires.
- An avalanche appears in the gas amplification zone around the anode wire.
- Newborn ions drift to cathode planes.

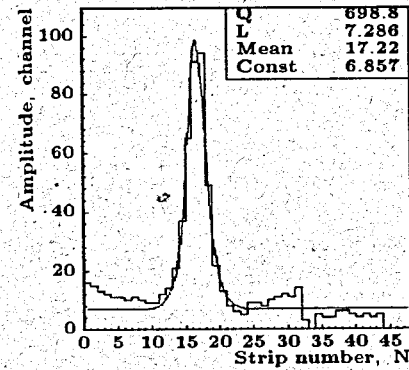


Figure 3: An example of strip amplitude peak.

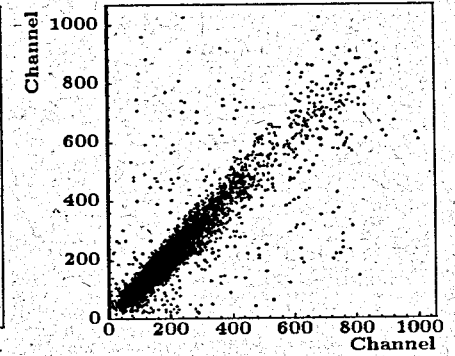


Figure 4: Dependence of charge induced on different cathode planes.

The electrostatic model is the simplest and adequate enough model of these processes. According to [3, 5] let us consider plane geometry with a "point-like" charge placed on the anode wire between two infinite cathode planes (see fig. 2, where  $L$  denotes an anode-cathode gap,  $a_i$  is a position of the  $i$ -th strip). The charge induced on the strip with the width  $w$  can be expressed as:

$$A_i = \frac{Q}{\pi} \arctan\left(\exp\left(\frac{\pi x}{2L}\right)\right) \Bigg|_{a_i}^{a_i+w} \quad (1)$$

In the frame of this model it can be inferred that:

- Charges induced on the both planes are equal.
- The total induced charge is proportional to one formed during the avalanche growth. Therefore, in the case of proportional chambers, it has to be proportional to the number of electrons getting to the anode wire.

However, several deviations from this idealized model can occur in real experiments. The most important of them are amplitude peak extension and difference of charges induced on adjacent surfaces. These deviations are

caused by capacitive mutual influence of strips, possible different resistance of cathode surfaces and work of cathode read-out electronics [6].

A typical example of the strip amplitude peak in chamber 4 is shown in fig. 3. This peak is fitted by a curve given in equation (1) plus  $C$  — a constant, corresponding to the pedestal (the level of noise). Free parameters are  $Q, L, X_{mean}, C$ . The double amplitude peak extension is clearly seen (obtained value of  $L = 7.268$  is roughly twice greater than the gap of chamber 4). The simplest change of the electrostatic model for accounting for this extension is correction of the parameter  $L$  in (1) for detected amplitude.

As was mentioned above, charges, induced on adjacent surfaces, are not exactly equal but only proportional in real experiments. This is just the case of the ARES facility. Figure 4 demonstrates this dependence of induced charges for strip chamber 4. The dispersedness around linear dependence is caused by the nature of physical processes in proportional chambers.

We also propose to use TIC information for additional analysis of complicate events. Let us consider once again the work of the proportional chamber [7]. Figure 5 shows track passing through a chamber at the angle  $\alpha$  to the anode wire. Electrons, formed outside an imaginary collection zone, are captured by electronegative admixtures during their drift to the anode wire. On the other hand, electrons, formed inside this zone, produce avalanches. Thus the total induced charge is proportional to the track path in the electron collection zone. This model is confirmed in fig. 6, where experimental dependence of TIC on the track path in the electron collection zone is plotted. A cluster of points in the region 0.4 cm is caused by the fact that the majority of tracks cross the chamber almost perpendicularly to anode wires. Thus, if the total charge is given, it is possible to approximate track inclination to the anode wire (to the  $Z$ -axis).

Note that we use the most obvious formula to calculate the charge induced on the strip surface:

$$Q = \sum_{i=-2}^2 A_i. \quad (2)$$

### 3 Algorithms of $Z$ -coordinate reconstruction

A standard procedure of  $Z$ -coordinate reconstruction of multitrack events in strip chambers consists of the following steps:

1. Peaks of strip amplitudes on each surface are searched for and strip coordinates of avalanches are determined.

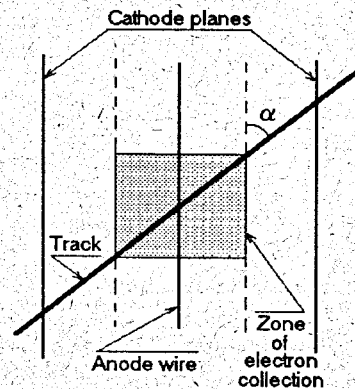


Figure 5: Track passing through strip proportional chamber.

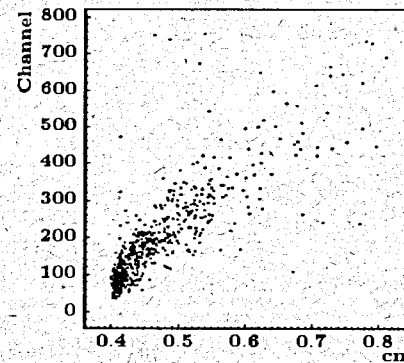


Figure 6: An experimental dependence of total induced charge on track path in electron collection zone.

2. Joining strip coordinates of avalanches with angles of hit anode wires, all possible  $Z$ -identifications of hit anode wires are calculated ( $Z$ -points).
3.  $Z$ -points are joined with previously found  $XY$ -tracks to get spatial  $SZ$ -lines ( $Z$ -identifications of tracks).
4. If there are more than one identification of an event, the most probable should be taken.

Now we will describe each step in detail.

#### 3.1 Determination of avalanche strip coordinate

The process of searching for avalanche strip coordinate begins with determination of an amplitude peak. Then, the coordinate of the strip with the maximum amplitude ( $A_0$ ) is taken, and it is corrected according to correlation with amplitudes of the nearest 2 or 4 strips ( $A_i$ ). Thus, the formula of the avalanche coordinate looks as:

$$C = C_0 + \Delta(A_0, A_{\pm 1}, A_{\pm 2}) \cdot w, \quad (3)$$



here  $C_0$  is the coordinate of the strip with the maximum amplitude,  $\Delta$  describes the above-mentioned correction. There are a lot of different types of the function  $\Delta$ , some of them are described in [3]. We adduce two most popular:

$$\Delta = \frac{\sum_{i=-2}^2 A_i \cdot i}{\sum_{i=-2}^2 A_i}; \quad (4)$$

$$\Delta = \frac{1}{2} \frac{A_1 - A_{-1}}{2A_0 - (A_1 + A_{-1})}. \quad (5)$$

Formula (4) determines the center of gravity of the peak, and formula (5) determines the so-called center of intensity. Obviously, in both formulae  $\Delta$  have linear dependence on  $i$ . These formulae are approximate and additional nonlinear corrections are often used (see [3, 5]) to improve resolution.

In the case of amplitude overflow in the peak maximum, we suggest that only amplitudes of peak "wings" be used, so the formula for  $\Delta$  turns to the following:

$$\Delta = \frac{A_2 + A_1 - A_{-1} - A_{-2}}{A_1 + A_{-1} - A_2 - A_{-2}}. \quad (6)$$

This modification allows us to keep  $Z$ -resolution in the case of amplitude overflow.

It is also clearly seen that formulae (5), (6) are strip amplitude baseline independent:

$$A_i = A_i + const \quad \forall i. \quad (7)$$

This fact makes them less sensible to the procedure of pedestal determination.

### 3.2 Formation of $Z$ -points

The next step after searching for strip coordinates of avalanches is determination of anode wire  $Z$ -identifications. To do it we must correctly join peaks on two adjacent surfaces with hit anode wires. We will call such a group a  $Z$ -point. There is no problem in the case of 1-prong events (see fig. 1). But for 3-prong events there are three peaks of a strip amplitude on each surface, thus they produce  $3 \cdot 3 \cdot 2 = 18$  candidates for  $Z$ -points.

To reject false  $Z$ -points we suggest the following method. Since we have two strip coordinates of an avalanche, we can find its azimuthal coordinate using the formula:

$$\Phi_{strip} = \frac{(Z_{02} - Z_{01}) + (DZ_2 \cdot C_2 - DZ_1 \cdot C_1)}{DZD\Phi_2 - DZD\Phi_1}. \quad (8)$$

Here  $Z_{0i}$  denotes  $Z$ -coordinates of crossing of the first anode wire centers with the first cathode strip centers on different surfaces;  $DZ_i$  stands for  $Z$  change when one goes to the next strip;  $DZD\Phi$  denotes  $Z$  increasing when one turns 1 radian along the strip, and  $C_i$  denotes the strip coordinate of the avalanche.

If the chamber works with the absolute accuracy,  $\Phi_{strip}$  simply equals  $\Phi_{anode}$ , determined from the azimuth of the anode wire. For real detectors the value

$$\Delta\Phi = \Phi_{strip} - \Phi_{anode}$$

has some distribution, whose width characterizes resolution of the device. So, obviously, false  $Z$ -points can be rejected according to the criterion:  $\Delta\Phi < 3.5\sigma_\Phi$ .

The same method can be applied to information about the total charges induced on different cathode surfaces. Figures 7 and 8 demonstrate usefulness of TIC information. Fig. 7 shows the distribution of  $\Delta\Phi$  for 3-prong events without charge cut (without requesting of charge proportionality on adjacent surfaces). One can see that even after  $\Delta\Phi$  cut besides true  $Z$ -points (a region of the peak), there are a lot of false  $Z$ -points distributed uniformly. In this case relation between true and false  $Z$ -points (signal/background ratio) can be measured as the peak height divided by the background constant. Fig. 8 shows the dependence of the signal/background ratio on cut on charge difference. So false  $Z$ -identifications can also be rejected according to the criterion:  $\Delta Q = |Q_1 - k_Q \cdot Q_2| < 3.5\sigma_Q$ .

### 3.3 Search for $SZ$ -lines

After we have found  $Z$ -points at separate chambers, it is necessary to connect them with profound  $XY$ -tracks, and thus with each other. We will call this procedure building of  $SZ$ -lines ( $Z$ -identification of tracks).

In the case of a uniform magnetic field, the track is a helix. Therefore the  $Z$ -coordinate of the track is proportional to its path from the vertex ( $Z_0$ ) to the chamber:

$$Z_i = Z_0 + kS_i. \quad (9)$$

Here  $Z_i$  is the  $Z$ -coordinate at the  $i$ -th chamber,  $Z_0$  is the coordinate of the track in the vertex,  $k$  is the track slope to the  $Z$  axis,  $S_i$  is the path from the vertex to the  $i$ -th chamber in  $XY$  plane. It is possible that some anode wires will have more than one  $Z$ -identification, and moreover, all of these identifications may be false. The simplest way is to try all these possibilities, including absence of any identifications, build all possible  $SZ$ -lines, and

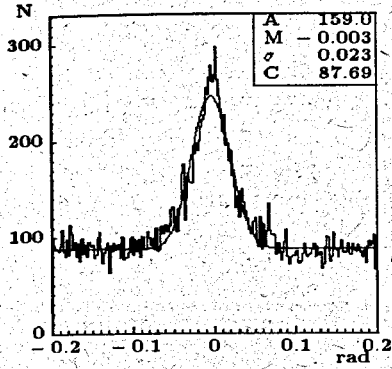


Figure 7: Histogram of  $\Delta\Phi$  for 3-prong events.

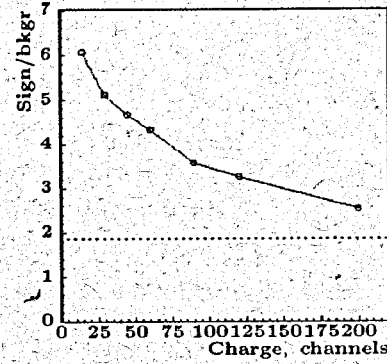


Figure 8: Signal/background ratio vs cut on charge difference.

exclude the worst identifications according to the  $\chi^2$ -criterion.

To determine parameters  $Z_0, k$  for the chosen combination of  $Z$ -points the least square method is used:

$$\mathcal{L}_{SZ} = \sum_i \frac{(Z_i - (Z_0 + kS_i))^2}{\sigma_{sz}^2}. \quad (10)$$

It is obviously linear.

Again, we can use charge information. As we found out in section 2, the charge is proportional to the path of a particle in the electron collection zone:

$$Q = \alpha_i s = \alpha_i s_{xy} \sqrt{1 + k^2}. \quad (11)$$

Here  $s$  is the full track path in the electron collection zone,  $s_{xy}$  is its projection onto the  $XY$ -plane. To use this fact, we add charge dependent part to the functional (10):

$$\mathcal{L}_{Qk} = \sum_i \frac{(Q_i - \alpha_i s_{xy} \sqrt{1 + k^2})^2}{\sigma_{Qk}^2}. \quad (12)$$

Coefficients  $\alpha_i$  and  $\sigma_{Qk}$  are obtained from the calibration procedure.

Though the full functional

$$\mathcal{L} = \mathcal{L}_{SZ} + \mathcal{L}_{Qk} \quad (13)$$

is not linear, it allows us to calculate  $\chi^2$  of an  $SZ$ -line even if it consists only of two  $Z$ -points. This feature is extremely important for the ARES facility because of its not very high efficiency.

During this stage of event  $Z$ -coordinate reconstruction, we can reject impossible  $SZ$ -lines using the criterion:

$$\chi^2 \leq \chi_{cut}^2. \quad (14)$$

### 3.4 Final event $Z$ -identification

When all  $SZ$ -lines are found, it is possible that some tracks have several identifications. Some of the tracks can share the same  $Z$ -point and vice versa, several points may not belong to any track. Though this is possible in principle, these identifications have low probability in practice. In any case our algorithm has to take into account such possibility. For most events it is resolved by the  $\chi^2$ -criterion. In other cases it is quite reasonable to use the method of maximum probability.

To determine the probability of  $Z$ -identification we suggest the following method that uses information about an angle of track slope to the  $Z$ -axis, derived from the total induced charge (see sect. 2).

Let us denote by  $p_{peak}, p_{point}, p_{line}$  — probabilities of peak,  $Z$ -point and  $SZ$ -line to be true, and by  $q_{peak}, q_{point}, q_{line}$  — that they are false. Let us denote also by  $p_{peak12}$  probability of two true peaks joining to give true  $Z$ -point. The probability of the inverse case is  $q_{peak12}$ .

A  $Z$ -point is characterized by five variables (only three of them are independent): azimuthal angle  $\Phi$ , avalanche coordinates on adjacent cathode surfaces  $C_1, C_2$  and charges induced on both surfaces  $Q_1, Q_2$ . Quantities  $\Delta\Phi = \Phi_{strip} - \Phi_{anode}$  and  $\Delta Q = Q_1 - k_Q Q_2$  have gaussian distribution for true  $Z$ -points, and they are obviously independent. So the value of  $\mathcal{F} = \Delta\Phi \cdot \Delta Q$  is distributed as product of two gaussians:

$$P_{true}(\mathcal{F}) = \frac{1}{2\pi\sigma_\Phi\sigma_Q} \exp\left(-\frac{(\Delta\Phi)^2}{2\sigma_\Phi^2} - \frac{(\Delta Q)^2}{2\sigma_Q^2}\right). \quad (15)$$

Consider the distribution of  $\mathcal{F}$  for false  $Z$ -points. It is clear, that random correlation of two peak-center coordinates and anode wire coordinates gives a uniform distribution of  $\Delta\Phi$ . The distribution of  $\Delta Q$  can be found from calibration. Thus:

$$P_{false}(\mathcal{F}) = \frac{1}{2\pi} \cdot P_{false}(\Delta Q). \quad (16)$$

Let we have the value of  $\mathcal{F}$  for the particular point and we want to find the probability that it is true while having an alternative hypothesis that it is false. It is obvious that

$$\begin{cases} \frac{p_{peak12}}{q_{peak12}} = \frac{P_{true}(\mathcal{F})}{P_{false}(\mathcal{F})}; \\ p_{peak12} + q_{peak12} = 1. \end{cases} \quad (17)$$

From this system we obtain:

$$\begin{cases} p_{peak12} = \frac{P_{true}(\mathcal{F})}{P_{true}(\mathcal{F}) + P_{false}(\mathcal{F})}; \\ q_{peak12} = \frac{P_{false}(\mathcal{F})}{P_{true}(\mathcal{F}) + P_{false}(\mathcal{F})}. \end{cases} \quad (18)$$

Consider  $Z$ -identification of a separate strip chamber. We will assume that tracks do not share points in the  $XY$ -plane. Therefore, if two  $Z$ -points do not share peaks of strip amplitudes, they are independent. If they do share, this fact must decrease the probability of the identification. So the probability of the particular  $Z$ -identification on the chamber looks like:

$$P_{chamber} = q_{peak}^{N_{peak0}} \cdot p_{peak(1)}^{N_{peak1}} \cdot p_{peak(2)}^{N_{peak2}} \cdot \dots \cdot \prod_{Z_{in}} p_{peak12} \cdot \prod_{Z_{out}} q_{peak12}. \quad (19)$$

In this formula we denote by  $N_{peak0}$  the number of peaks that are not included into the identification,  $N_{peak1}$  — included only ones, etc; by  $p_{peak(i)}$  — the probability that the peak is used  $i$  times.  $Z_{in}$  means the set of points included into the identification as true, and  $Z_{out}$  stands for the set of false  $Z$ -points. We should mention here that the fact we did not use  $Z$ -points rejected by restrictions  $\Delta\Phi < 3.5\sigma_{\rho_{hi}}$  and  $\Delta < 3.5\sigma_Q$  practically does not have influence as for these points  $q_{peak12} \approx 1$ .

Almost the same reasoning can be applied to  $SZ$ -lines probabilities. Thus, the probability of event identification is given by a formula:

$$P_{ident} = \prod_{i=1}^3 P_{chamber}^i \prod_{j=1}^N P_{line}^j, \quad (20)$$

here  $P_{line}^j$  denotes the probability of the  $SZ$ -line.

Therefore, to chose final event identification, it is necessary to look over all possible identifications and find one with the greatest probability:

$$\mathcal{P} = \max_{\{ident\}} P_{ident}. \quad (21)$$

Table 1: Resolution of strip chambers.

N chamber	$\sigma_\phi$ (rad)	$\sigma_Q$ (channel)	$\sigma_Z$ (mm)
1	$1.16 \cdot 10^{-2}$	17.5	2.1
4	$1.18 \cdot 10^{-2}$	32.6	2.1
9	$0.78 \cdot 10^{-2}$	101.0	2.1

## 4 Conclusion

The results of the application of the suggested method are given in table 1. For  $Z$  resolution determination we use a standard method, described in [8]. It is seen that the accuracy of the ARES strip chambers is comparatively low. This fact can be explained both by the reasons described in sect. 2 and by not optimal parameters of chambers, for example, the ratio of the strip width to the anode-cathode gap.

The use of TIC information leads to reliable  $Z$ -identifications. It also allows one to increase significantly the speed of calculations by rejecting false points. The developed methods of  $Z$ -reconstruction work under hard conditions of the ARES facility quite successfully.

## References

- [1] V.A. Baranov et al., Nucl. Instr. and Meth. 203 (1982) 291.
- [2] V.A. Baranov et al., J. Phys. G: Nucl. Part. Phys. 17 (1991) S57.
- [3] C. Grab, Search for  $\mu \rightarrow 3e$  decay. Dissertation, Universitat Zürich, 1985.
- [4] G. Charpak and F. Sauli, Nucl. Instr. and Meth. 113 (1973) 381.
- [5] I. Endo et al., Nucl. Instr. and Meth. 188 (1981) 51.
- [6] E. Gatti et al., Nucl. Instr. and Meth. 163 (1979) 83.
- [7] A. Glazov et al., JINR Commun. E10-91-507, Dubna (1991).
- [8] F. Piuz et al., Nucl. Instr. and Meth. 196 (1982) 451.

Received by Publishing Department  
on April 8, 1993.